J|A|C|S
ARTICLES

Published on Web 08/21/2008

Polarization Energies in Oligoacene Semiconductor Crystals

Joseph E. Norton and Jean-Luc Brédas*

School of Chemistry and Biochemistry and Center for Organic Photonics and Electronics, Georgia Institute of Technology, Atlanta, Georgia 30332-0400

Received March 10, 2008; E-mail: jean-luc.bredas@chemistry.gatech.edu

Abstract: Characterization of the electronically polarized environment and the nuclear relaxation that accompanies charge carriers is fundamental to charge transport in crystalline, polycrystalline, and amorphous organic solids. To study the polarization effects of localized charged carriers, we use quantum/classical QM/MM approaches with charge redistribution and polarizable force field schemes and apply them to crystals of naphthalene through pentacene. We describe the results of a comprehensive investigation of the electronic polarization energies in molecular crystal structures of these oligoacenes and discuss as well the evolution of the nuclear relaxation energies calculated for model oligoacene systems.

I. Introduction

An understanding of charge transport in organic crystals and amorphous organic solids requires knowledge of the distributions of site and state energies that occur due to the polarization of the charge carrier environment. Molecular and crystal packing structure and physical disorder in crystalline and amorphous organic solids are key factors in determining the distributions of polarization energies that impact charge transport. Molecules in organic solids interact through weak intermolecular van der Waals interactions, which allow charge carriers to become strongly localized on individual sites or on a small number of molecules.[1] Electron and hole charge carriers exist as polaron-type quasi-particles characterized by *instantaneous* intra- and intermolecular electronic polarization of neighboring molecules; at longer times, nuclear relaxations also play a role. The polarization energy associated with this state is analogous and comparable to the solvation energy of ions in solution.[2]

Since the polarization energy associated with a given site depends on its local environment, it is of practical importance to be able to account for the detailed molecular and electronic structure of the medium surrounding a charge carrier. As polarization effects in solids are expected to extend over several nanometers from the charge core,[2] the ability to model long-range interactions in crystalline and amorphous materials (where energetic disorder and electronic and structural defects exist) is especially important. Here, we present a comprehensive study of the electronic polarization energies within molecular crystal structures of oligoacenes ranging from naphthalene to pentacene.

Linear oligoacenes are a class of polycyclic aromatic hydrocarbons that have become prototypical models for studying charge carrier energetics and dynamics in organic molecular crystals.[2–7] The potential for oligoacenes in organic electronic applications such as field-effect transistors and light-emitting diodes[8] and solar cells[9,10] has stimulated interest in their fundamental electronic and geometric properties. Determining the polarization energy of localized charges in oligoacene crystals has recently been of both experimental[1,3,11–15] and theoretical[16–21] interest. In particular, polarization energies of charged electronic states near idealized grain boundaries in pentacene crystals were shown to create intrinsic energy barriers or trapping centers that can depend on crystal structure and film growth conditions.[16] In other studies, the electronic properties of ion clusters of naphthalene,[1,12,14] anthracene,[14] and tetracene[13]

(1) Saigusa, H.; Lim, E. C. *J. Phys. Chem.* **1994**, *98*, 13470–13475.
(2) Silinsh, E. A.; Čápek, V. *Organic Molecular Crystals: Interaction, Localization, and Transport Phenomena*; American Institute of Physics: New York, 1994.
(3) Pope, M.; Swenberg, C. E. *Electronic Processes in Organic Crystals and Polymers*; Oxford University Press: New York, 1999.
(4) Brédas, J. L.; Calbert, J. P.; da Silva Filho, D. A.; Cornil, J. *Proc. Natl. Acad. Sci. U.S.A.* **2002**, *99*, 5804–5809.
(5) Bendikov, M.; Wudl, F.; Perepichka, D. F. *Chem. Rev.* **2004**, *104*, 4891–4945.
(6) Brédas, J. L.; Beljonne, D.; Coropceanu, V.; Cornil, J. *Chem. Rev.* **2004**, *104*, 4971–5003.
(7) Coropceanu, V.; Cornil, J.; da Silva Filho, D. A.; Olivier, Y.; Silbey, R.; Brédas, J. L. *Chem. Rev.* **2007**, *107*, 926–952.
(8) Anthony, J. E. *Chem. Rev.* **2006**, *106*, 5028–5048.
(9) Yoo, S.; Domercq, B.; Kippelen, B. *Appl. Phys. Lett.* **2004**, *85*, 5427–5429.
(10) Yoo, S.; Domercq, B.; Kippelen, B. *J. Appl. Phys.* **2005**, *97*, 103706/1–103706/9.
(11) Sato, N.; Seki, K.; Inokuchi, H. *J. Chem. Soc., Faraday Trans. 2* **1981**, *77*, 1621–1633.
(12) Song, J. K.; Han, S. Y.; Chu, I.; Kim, J. H.; Kim, S. K.; Lyapustina, S. A.; Xu, S.; Nilles, J. M.; Bowen, K. H., Jr *J. Chem. Phys.* **2002**, *116*, 4477–4481.
(13) Mitsui, M.; Ando, N.; Nakajima, A. *J. Phys. Chem. A* **2007**, *111*, 9644–9648.
(14) Mitsui, M.; Kokubo, S.; Ando, N.; Matsumoto, Y.; Nakajima, A.; Kaya, K. *J. Chem. Phys.* **2004**, *121*, 7553–7556.
(15) Sato, N.; Inokuchi, H.; Silinsh, E. A. *Chem. Phys.* **1987**, *115*, 269–277.
(16) Verlaak, S.; Heremans, P. *Phys. Rev. B: Condens. Matter Mater. Phys.* **2007**, *75*, 115127/1–115127/14.
(17) Soos, Z. G.; Tsiper, E. V.; Pascal, R. A., Jr *Chem. Phys. Lett.* **2001**, *342*, 652–658.
(18) Tsiper, E. V.; Soos, Z. G. *Phys. Rev. B: Condens. Matter Mater. Phys.* **2001**, *64*, 195124/1–195124/12.
(19) Knowles, D. B.; Munn, R. W. *J. Mater. Sci.: Mater. Electron.* **1994**, *5*, 89–93.
(20) Eisenstein, I.; Munn, R. W. *Chem. Phys.* **1983**, *77*, 47–61.
(21) Castet, F.; Aurel, P.; Fritsch, A.; Ducasse, L.; Liotard, D.; Linares, M.; Cornil, J.; Beljonne, D. *Phys. Rev. B: Condens. Matter Mater. Phys.* **2008**, *77*, 115210/1–115210/14.

were used to understand the relationship between charges in finite-sized clusters and organic solids.

In the present study, we use hybrid quantum mechanical (QM) and molecular mechanical (MM) methods to describe the electronic polarization energy in oligoacene crystal structures. It was shown that quantum corrections to static classical polarization energies come mainly from dynamical polarization contributions of the molecular ion itself,[22,23] and these effects can be captured by treating the charge carrier quantum mechanically and the environment with molecular mechanics. Polarization energies are calculated using QM/MM methods within a charge fluctuation scheme, where atomic charges are allowed to vary depending on the molecular structure of the environment. We also considered QM/MM methods with a polarizable force field based on distributed multipoles and QM methods with a polarizable continuum model (PCM) where the environment is treated as a dielectric continuum instead of explicitly accounting for molecular crystal structure. In addition, we investigated the total relaxation energies for QM/MM models of the naphthalene crystal to provide an estimate of the impact of intermolecular nuclear (geometric) relaxation.

II. Methodology

Hybrid quantum mechanical and molecular mechanical models are used to partition large chemical systems into an electronically important region that requires a quantum mechanical treatment and a perturbative region that permits a classical description.[24] Hybrid QM/MM methods were applied to many problems involving chemical reactivity in the presence of solvents and biochemical applications such as enzymatic catalysis.[25] The accuracy of QM approaches combined with the computational efficiency of MM force fields offers an attractive approach to studying charge polarization and geometric and electronic reorganization in polymer systems and organic solids. A key issue in obtaining accurate results with QM/MM methods is the proper definition of the interface between the QM and MM regions. For crystalline and amorphous solids, it is often the case that the QM and MM regions are not covalently linked, and the problem of the QM/MM interface becomes one of appropriately describing nonbonding interactions between QM and MM atoms. The interaction between the QM and MM regions must also be appropriately defined to account for polarization effects such as charge reorganization.

Here, the ONIOM[26–34] QM/MM method implemented in Gaussian 03[35] is used where the total energy of the system is obtained from the equation:

$$E_{\mathrm{ONIOM}} = E_{\mathrm{MM,real}} - E_{\mathrm{MM,model}} + E_{\mathrm{QM,model}} \quad (1)$$

where *real* refers to the entire system and *model* refers to the subregion that, in this case, will be treated with QM methods. Quantum mechanical calculations were carried out using the B3LYP hybrid functional[36–38] and 6-31G+G(d) basis set. Two schemes were employed to allow for polarization of the surrounding medium and the charge carrier. In both approaches, the atomic charges assigned to the MM region are electronically embedded into the core Hamiltonian, effectively allowing the MM region to polarize the QM region. In the first approach, the electrostatic charges of the MM region are obtained using the UFF force field[39] and the self-consistent charge equilibration (QEq) scheme proposed by Rappé and Goddard.[40] The QEq method implements a variable-charge model where the partial atomic charges depend on molecular geometry by requiring the chemical potential at each atom to be equivalent. Similar charge fluctuation approaches were implemented to account for classical polarization effects in solute−solvent systems[41–43] and hydrogen bonding in water and protein−ligand interactions.[44] To allow the surrounding medium to polarize the model region in conjunction with the QEq approach, the CHELPG[45] charges of the QM region are iteratively fed back into the *model* MM region of the calculations until convergence of the energy ($\Delta E < 1 \times 10^{-6}$ au) is achieved. During this process, the surrounding MM region maintains a net neutral charge while equilibration occurs in the presence of the charged *model* QM/MM region. The changes in electron density within the QM region are reflected in the MM calculation to allow for back interaction with the electrostatic charge distribution of the environment.

The second approach uses the polarizable atomic multipole optimized energetics for biomolecular applications (AMOEBA)[46–48] force field implemented in TINKER version 4.2.[49] Each atom in this force field has a permanent partial charge, dipole, and quadrupole moment, and electronic many-body effects are represented using a self-consistent dipole polarization procedure.[46] Repulsion−dispersion interactions between pairs of nonbonded atoms are represented by a buffered 14−7 potential.[50] The polarizable force field was developed for use on naphthalene clusters; therefore, it was necessary for us to develop new multipole parameters for the neutral and ionic naphthalene molecules. The geometries and electronic structures of the naphthalene molecules were obtained from ab initio calculations at the MP2/6-311++G(2d,2p) level. Atomic charge, dipole, and quadrupole values were determined by distributed multipole analysis through the GDMA program.[51] To be consistent with parametrization procedures defined in the AMOEBA force field,[46] the atomic

(22) Čápek, V. *Czech. J. Phys.* **1978**, *B28*, 773–780.
(23) Silinsh, E. A.; Čápek, V.; Nedbal, L. *Phys. Status Solidi B* **1980**, *102*, K149–K152.
(24) Bakowies, D.; Thiel, W. *J. Phys. Chem.* **1996**, *100*, 10580–10594.
(25) Friesner, R. A.; Guallar, V. *Annu. Rev. Phys. Chem.* **2005**, *56*, 389–427.
(26) Maseras, F.; Morokuma, K. *J. Comput. Chem.* **1995**, *16*, 1170–1179.
(27) Humbel, S.; Sieber, S.; Morokuma, K. *J. Chem. Phys.* **1996**, *105*, 1959–1967.
(28) Martsubara, T.; Sieber, S.; Morokuma, K. *Int. J. Quantum Chem.* **1996**, *60*, 1101–1109.
(29) Svensson, M.; Humbel, S.; Froese, R. D. J.; Matsubara, T.; Sieber, S.; Morokuma, K. *J. Phys. Chem.* **1996**, *100*, 19357–19363.
(30) Svensson, M.; Humbel, S.; Morokuma, K. *J. Chem. Phys.* **1996**, *105*, 3654–3661.
(31) Dapprich, S.; Komáromi, I.; Byun, K. S.; Morokuma, K.; Frisch, M. J. *J. Mol. Struct.: THEOCHEM* **1999**, *461−462*, 1–21.
(32) Vreven, T.; Morokuma, K. *J. Comput. Chem.* **2000**, *21*, 1419–1432.
(33) Vreven, T.; Byun, K. S.; Komaromi, I.; Dapprich, S.; Montgomery, J. A., Jr.; Morokuma, K.; Frisch, M. J. *J. Chem. Theory Comput.* **2006**, *2*, 815–826.
(34) Morokuma, K. *Bull. Korean Chem. Soc.* **2003**, *24*, 797–801.
(35) Frisch, M. J.; et al. *Gaussian 03*, revision B.02; Gaussian, Inc.: Wallingford, CT, 2004.
(36) Becke, A. D. *Phys. Rev. A: At., Mol., Opt. Phys.* **1988**, *38*, 3098–3100.
(37) Becke, A. D. *J. Chem. Phys.* **1993**, *98*, 5648–5652.
(38) Lee, C.; Yang, W.; Parr, R. G. *Phys. Rev. B: Condens. Matter Mater. Phys.* **1988**, *37*, 785–789.
(39) Rappé, A. K.; Casewit, C. J.; Colwell, K. S.; Goddard, W. A., III; Skiff, W. M. *J. Am. Chem. Soc.* **1992**, *114*, 10024–10035.
(40) Rappé, A. K.; Goddard, W. A., III *J. Phys. Chem.* **1991**, *95*, 3358–3363.
(41) Field, M. J. *Mol. Phys.* **1997**, *91*, 835–845.
(42) Bryce, R. A.; Vincent, M. A.; Malcolm, N. O. J.; Hillier, I. H.; Burton, N. A. *J. Chem. Phys.* **1998**, *109*, 3077–3085.
(43) Bryce, R. A.; Vincent, M. A.; Hillier, I. H. *J. Phys. Chem. A* **1999**, *103*, 4094–4100.
(44) Illingworth, C. J. R.; Gooding, S. R.; Winn, P. J.; Jones, G. A.; Ferenczy, G. G.; Reynolds, C. A. *J. Phys. Chem. A* **2006**, *110*, 6487–6497.
(45) Breneman, C. M.; Wiberg, K. B. *J. Comput. Chem.* **1990**, *11*, 361–373.
(46) Ren, P.; Ponder, J. W. *J. Comput. Chem.* **2002**, *23*, 1497–1506.
(47) Ren, P.; Ponder, J. W. *J. Phys. Chem. B* **2003**, *107*, 5933–5947.
(48) Grossfield, A.; Ren, P.; Ponder, J. W. *J. Am. Chem. Soc.* **2003**, *125*, 15671–15682.
(49) Ponder, J. W. *TINKER: Software Tools for Molecular Design*, version 4.2; Washington University: St. Louis, MO, 2004.
(50) Halgren, T. A. *J. Am. Chem. Soc.* **1992**, *114*, 7827–7843.

multipoles were rotated from the global coordinate frame to a conventional local frame.

Dielectric continuum theories[52,53] are widely used to determine solvation energies in conjunction with quantum mechanical calculations due to the relatively low computational costs. In particular, the conductor-like polarizable continuum model (CPCM)[54–57] was successfully used in calculating solvation energies of neutral and ionic organic molecules.[58] The integral equation formalism model of the polarizable continuum model was also used to account for the effects of the crystal environment on electronic coupling parameters for anthracene and pentacene crystals.[59] In a similar approach, the condensed phase is treated here using the CPCM model with a molecular cavity built up from the united atom (UA0) model and a dielectric constant (ε) of 4.0 to represent a typical nonpolar insulating organic material.

The electronic polarization energy of the cation (P_+) is defined as the difference in energy between the ionization potential of the molecular system in the crystal (IP_{cry}) and the ionization potential of the molecular system in the gas phase (IP_{gas}), according to eqs 2, 3, and 4:

$$P_+ = IP_{cry} - IP_{gas} \quad (2)$$

$$IP_{gas} = E_{q(1),gas} - E_{q(0),gas} \quad (3)$$

$$IP_{cry} = E_{q(1),cry} - E_{q(0),cry} \quad (4)$$

where $E_{q(1)}$ and $E_{q(0)}$ denote the energies of the cation and neutral states, respectively, at either the gas-phase ground-state geometry or the crystal structure geometry. An analogous definition for anion polarization energy (P_-) is obtained by using electron affinities instead of ionization potentials. In general, the chosen conventions result in negative cation and anion polarization energies so as to reflect the stabilizing nature of the interactions in the condensed phase.

III. Results and Discussion

Various two- and three-dimensional oligoacene clusters were selected to monitor the evolution of the polarization energy as a function of cluster size. Molecular crystal geometries were obtained from experimental crystal structures of naphthalene,[60] anthracene,[61] tetracene,[62] and pentacene.[63] Two-dimensional structures were constructed as single herringbone layers of molecules with a localized charge carrier surrounded by geometrically closed shells of molecules. Three-dimensional structures were constructed as spherical clusters of molecules with center-of-mass distances within a given radius from a central charge carrier.

Polarization energies were calculated using the QM/MM approach with a charge fluctuation model (QM/UFF); the QM/MM methods with a polarizable force field (QM/AMOEBA) and the polarizable continuum model were used for comparison. To explore the contribution of geometric relaxation to polarization effects, total relaxation energies were calculated for naphthalene clusters using the QM/UFF method.

A. Electronic Polarization Energies in Oligoacene Crystals. a. Two-Dimensional Structures. We first discuss single-layer clusters built from the naphthalene, anthracene, tetracene, and pentacene crystal structures. The results obtained at the QM/MM B3LYP/6-31+G(d)/UFF level are reported in Figure 1. Each data point represents the addition of shells of molecules corresponding to the incorporation of nearest neighbor and successive next-nearest neighbor interactions, as shown in Figure 1a for a single layer of naphthalene molecules with two molecular crystal shells surrounding a single-molecule core. The values for the infinite clusters are extrapolated in Figure 1c by considering simple linear fits of the polarization energy as a function of $N^{-1/2}$, which is proportional to the inverse radius of a single-layer cluster. For each oligoacene, the polarization energy of the anion charge carrier is larger than that of the cation, and polarization energies increase in absolute value with cluster size. The magnitude of the polarization energy increases quickly as the first couple of shells of molecules are added. Although full convergence of the polarization energy does not occur until a sufficient number of long-range interactions are included, we note that approximately 70−80% of the polarization energy is captured within the first two shells and 80−90% within the first three.

It is most interesting to point out that the convergence of the *differences* in polarization energies, or site energy differences, for adjacent molecules near the core of the cluster occurs for much smaller cluster sizes than does the magnitude of the polarization energy itself. For example, site energy differences in naphthalene and anthracene crystals should be zero, since both crystal structures contain two identical centrosymmetric molecules per unit cell. The site energy differences are calculated to be zero already for clusters containing three shells (37 molecules). Tetracene and pentacene crystal structures contain two slightly nonequivalent molecules per unit cell resulting in site energy differences on the order of 0.01−0.02 eV for large clusters. We emphasize that with regard to charge carrier transport in crystalline or amorphous organic materials, it is the site energy differences that matter, not the absolute value of the polarization energies. Thus, these results are important as they demonstrate that calculations on relatively small cluster sizes are sufficient to provide accurate site energy differences.

It is often assumed that P_- and P_+ are approximately equal, especially in models where molecular structure is neglected and molecules are reduced to individual polarizable points. However, molecular packing determines the exact nature of the interactions that occur immediately near a charge carrier. A demonstration of this arises in the observed asymmetry in anion (P_-) and cation (P_+) polarization energies for layers of oligoacenes; P_- is larger than P_+. It is well-known that the herringbone crystal packing structure of oligoacenes generates interactions where the hydrogen atoms are protruding into the aromatic π-system of neighboring molecules, causing the partial positive charges on the hydrogens to reside close to the partial negative charges on the carbons; intermolecular C−H distances in oligoacenes are ~2.7−2.8 Å and distances from a given hydrogen to the molecular plane of a nearest neighbor can be as short as 2.6 Å. As a result, *differences in how the atomic charges are distributed within the anion and cation molecules will have an effect on*

(51) Stone, A. J. *J. Chem. Theory Comput.* **2005**, *1*, 1128–1132.
(52) Cramer, C. J.; Truhlar, D. G. *Chem. Rev.* **1999**, *99*, 2161–2200.
(53) Tomasi, J.; Persico, M. *Chem. Rev.* **1994**, *94*, 2027–2094.
(54) Andzelm, J.; Kolmel, C.; Klamt, A. *J. Chem. Phys.* **1995**, *103*, 9312–9320.
(55) Barone, V.; Cossi, M. *J. Phys. Chem. A* **1998**, *102*, 1995–2001.
(56) Cossi, M.; Rega, N.; Scalmani, G.; Barone, V. *J. Comput. Chem.* **2003**, *24*, 669–681.
(57) Klamt, A.; Schueuermann, G. *J. Chem. Soc., Perkin Trans. 2* **1993**, 799–805.
(58) Takano, Y.; Houk, K. N. *J. Chem. Theory Comput.* **2005**, *1*, 70–77.
(59) Lipparini, F.; Mennucci, B. *J. Chem. Phys.* **2007**, *127*, 144706/1–144706/6.
(60) Brock, C. P.; Dunitz, J. D. *Acta Crystallogr., Sect. B* **1982**, *B38*, 2218–2228.
(61) Brock, C. P.; Dunitz, J. D. *Acta Crystallogr., Sect. B* **1990**, *B46*, 795–806.
(62) Holmes, D.; Kumaraswamy, S.; Matzger, A. J.; Vollhardt, K. P. C. *Chem.−Eur. J.* **1999**, *5*, 3399–3412.
(63) Siegrist, T.; Kloc, C.; Schön, J. H.; Batlogg, B.; Haddon, R. C.; Berg, S.; Thomas, G. A. *Angew. Chem., Int. Ed.* **2001**, *40*, 1732–1736.

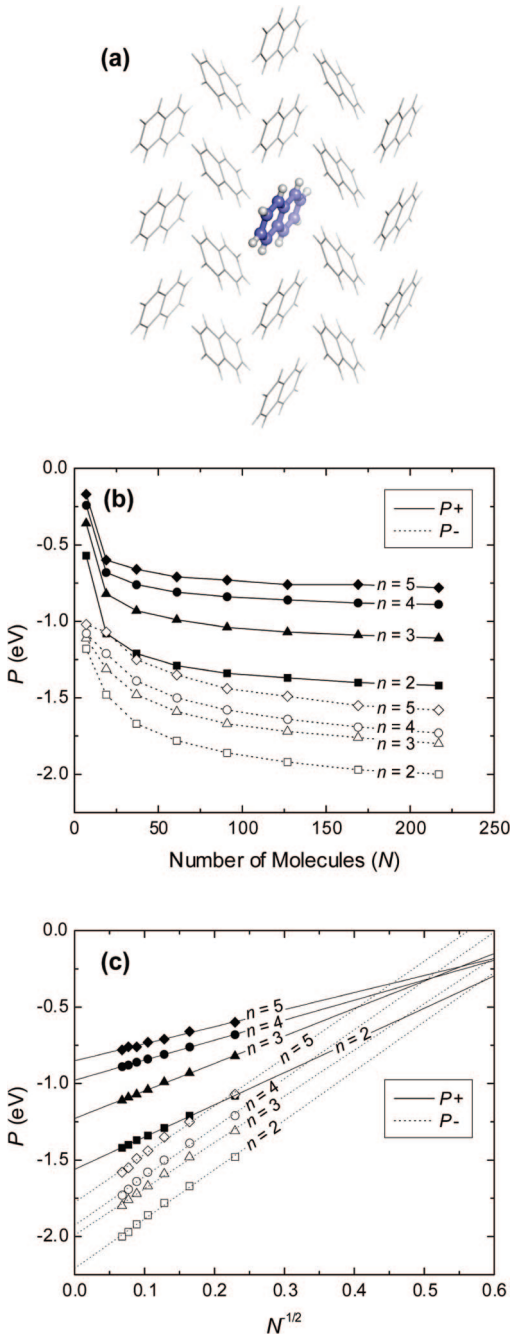

Figure 1. (a) Two-dimensional single-layer naphthalene cluster consisting of a single-molecule core surrounded by two molecular crystal shells corresponding to nearest and next-nearest neighbors. The ball and stick model represents the region treated with QM at the center, and the wire model represents the region treated with MM. (b) Polarization energies of single-layer oligoacene clusters calculated at the B3LYP/6-31+G(d)/UFF QM/MM level. Polarization energies are reported as a function of the number of molecules (N), and each data point represents the addition of a full shell of molecules. Values of n specify the total number of fused benzene units. (c) Evolution of $P_{\pm}$ as a function of $N^{-1/2}$ with linear fits shown as straight lines.

these intermolecular interactions. In the oligoacene cations, partial positive charges are on the hydrogen atoms while the carbon atoms retain very small partial negative charges. In the anion, the hydrogens retain substantial partial positive charges while the carbons accommodate larger partial negative charges, resulting in stabilizing intermolecular C−H interactions and larger polarization energies with respect to the cation. These differences are shown in Figure 2 for the cases of naphthalene and pentacene.

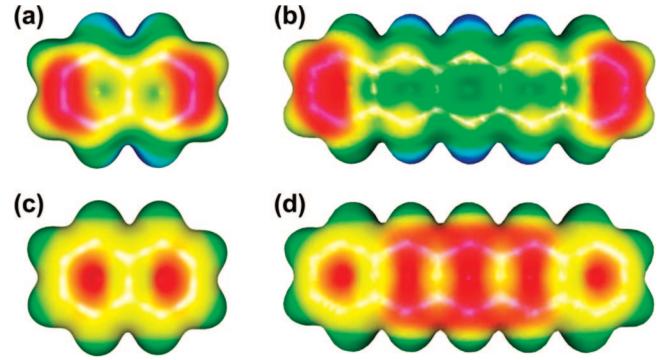

Figure 2. Electrostatic potential surface of the naphthalene molecule bearing a positive (a) or negative (c) charge embedded in a spherical cluster with $R = 25.0$ Å and the pentacene molecule bearing a positive (b) or negative (d) charge embedded in a spherical cluster with $R = 31.3$ Å. Negative electrostatic potential is indicated in red, and positive electrostatic potential is indicated in blue.

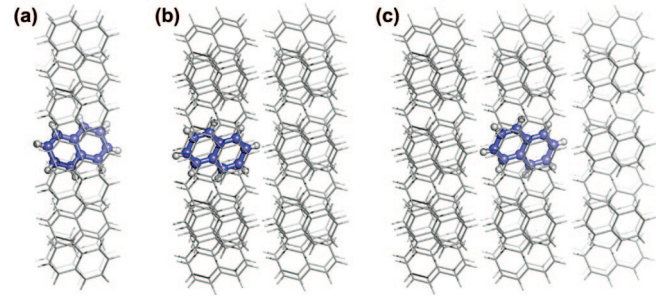

Figure 3. (a) Single-layer naphthalene cluster approximately 2 × 3 unit cells along the a and b crystal directions with corresponding (b) three-dimensional double- and (c) triple-layer crystal structures expanded along the c direction.

b. Three-Dimensional Structures. We now turn to interlayer contributions to the polarization energy. These are investigated initially by looking at three-dimensional (3D) structures generated from oligoacene crystals. First, single-, double-, and triple-layer structures of naphthalene clusters were generated. A single (2D) layer approximately 2 × 3 unit cells along the a and b crystal directions of naphthalene is shown in Figure 3a, with 3D double- and triple-layer structures expanded along the c direction, shown in Figure 3b,c. For the naphthalene structures shown in Figure 1, P_+ evolves from −1.07 eV in a single 2D layer to −1.32 and −1.51 eV for 3D double and triple layers. Polarization of the anion is noticeably less affected by interlayer contributions, as P_- is −1.45, −1.52, and −1.57 eV for single, double, and triple layers, respectively. This is an effect of molecular and crystal structure that causes P_+ and P_- to begin to converge to a similar value, indicating the larger three-dimensional cluster sizes reduce the differences between cation and anion polarization energies.

Polarization energies were then calculated for *spherical* 3D structures (Figure 4a) centered at a single-molecule core and consisting of molecules within a given radius determined by center-of-mass distances. Polarization energies of the oligoacenes are plotted in Figure 4b as a function of the number of molecules in each sphere with a given radius. The values for the infinite clusters are extrapolated in Figure 4c using linear fits of the polarization energy as a function of $N^{-1/3}$, which is proportional to the inverse radius of a spherical cluster. The

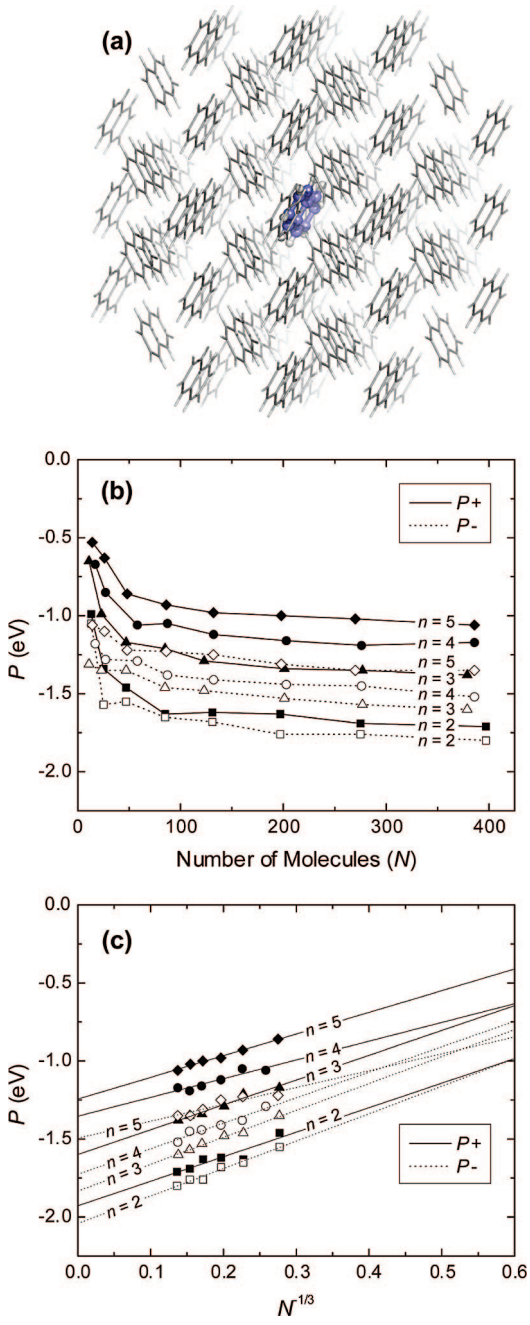

Figure 4. (a) 3D naphthalene cluster consisting of a single-molecule core surrounded by molecules within a center-of-mass distance of 15 Å. The ball and stick model represents the QM region treated with QM, and the wire model represents the region treated with MM. (b) Polarization energies of 3D oligoacene clusters calculated at the B3LYP/6-31+G(d)/UFF QM/MM level. Polarization energies are reported as a function of the number of molecules (N), and each data point represents a sphere of molecules within a given radius from the center-of-mass of a single-molecule core. Values of n specify the total number of fused benzene units. (c) Evolution of $P_{\pm}$ as a function of $N^{-1/3}$ with linear fits shown as straight lines.

magnitudes of the polarization energies are larger for smaller oligoacenes. Polarization of the anion remains stronger, as in the single-layer clusters; however, interlayer contributions bring the polarization energies closer by stabilizing the cation relative to the anion. Again, this effect is related to molecular crystal structure and how the atomic charges are distributed on the molecules, as discussed above. Thus, the specific relative packing of molecules from adjacent layers provides greater stabilization of the cation, as is evidenced by both the evolution of the polarization energy of naphthalene as a function of the number of layers and by the polarization energies of the oligoacene spherical clusters.

Table 1. Principal Components of the Quadrupole Moment (e Å^2) of Naphthalene Reported with Respect to the Normal (x), Long (y), and Medium (z) Molecular Axes

	charge	Θ_{xx}	Θ_{yy}	Θ_{zz}
MP2/6-311++G(2d,2p)[a]	0	−2.989	1.508	1.481
MP2/6-311++G(2d,2p)[a]	+1	−6.165	4.719	1.447
MP2/6-311++G(2d,2p)[a]	−1	−5.049	−5.049	−0.607
experimental[b]	0	−2.771	1.278	1.493

[a] Calculated multiple moments were determined by distributed multipole analysis of the calculated wave function using the GDMA program.[51] [b] Derived from theoretical calculations scaled to the experimental result of benzene; see ref 20.

c. Assessment of the Polarizable Force Field and Continuum Models. The QM/MM method with the AMOEBA polarizable force field uses a permanent partial charge, dipole, and quadrupole moment for each atom and relies on charge-induced dipole interactions to account for polarization. The parameters for the atomic multipoles were derived for naphthalene using a distributed multipole analysis, as described in the Methodology. For validation and comparison, the net principal components of the quadrupole moment of naphthalene derived from the calculated atomic multipole moments are reported in Table 1. The calculated quadrupole moment of the neutral molecule agrees well with other values reported in the literature. The principal components of the quadrupole moments calculated for the charged molecules are also listed in Table 1.

The total polarization energies obtained for naphthalene using the polarizable force field are displayed in Figure 5a,c. Linear extrapolations of $P_{\pm}$ for single-layer and spherical clusters are displayed in Figure 5b,d, respectively. The net polarization energy is composed of interactions with permanent multipoles ($P_{\text{Multipole},\pm}$) and induced dipole moments ($P_{\text{Induced Dipole},\pm}$), and the quantum mechanical contributions ($P_{\text{QM},\pm}$) of the charge carrier; we also display these component polarization energies in Figure 5a,c. The $P_{\text{QM},\pm}$ contributions include the dynamical polarization of the charge carrier and were estimated to be 0.05−0.4 eV for oligoacenes.[23] With QM/AMOEBA, the total P_+ values are larger than P_- values for both 2D single-layer and 3D spherical clusters, shown in Figure 5a,c, respectively. When extrapolated to infinite clusters, P_+ is –1.21 and –1.42 eV for two- and three-dimensional clusters, respectively. P_- is 0.05 eV for a single-layer cluster, while the corresponding value for the spherical clusters increases to –0.69 eV, indicating substantial interlayer contributions to stabilization of the anion. For both single-layer and three-dimensional structures, the multipole interactions and QM contributions counteract the interactions with induced dipoles for the union, resulting in smaller net P_- magnitudes. The opposite occurs for the cation, and all interactions work in concert to give larger net P_+ magnitudes. For three-dimensional structures, the contributions from multipole interactions are approximately 0.24 eV for the anion and –0.14 eV for the cation. The corrections coming from the QM treatment of the charged species, $P_{\text{QM},\pm}$, are on the order of 0.2 eV, which is larger than previous estimates of 0.05 eV for naphthalene but not as large as estimated values (0.4 eV) for pentacene.[23]

In comparison to the charge fluctuation model, the AMOEBA force field provides lower polarization energies. Since charge redistribution is a major contribution to the polarizability of

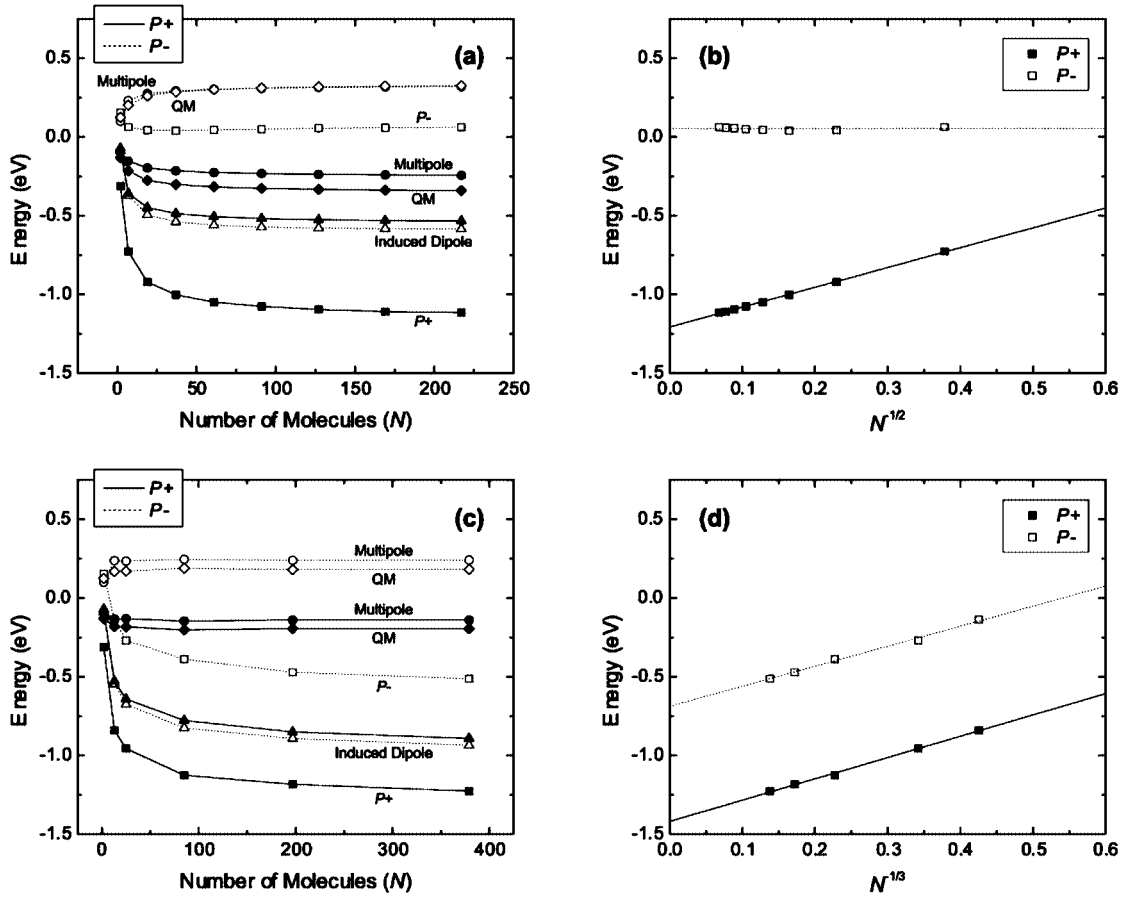

Figure 5. Total and component polarization energies of (a) single-layer and (c) three-dimensional clusters of naphthalene molecules calculated with QM/MM at the B3LYP/6-31+G(d):AMOEBA level. Linear fits of the evolution of $P_{\pm}$ as a function of (b) $N^{-1/2}$ and (d) $N^{-1/3}$ for 2D and 3D clusters, respectively.

conjugated molecules and the QM/AMOEBA method neglects inter- and intramolecular charge redistribution, this underestimation can be easily understood. In addition, an advantage of the QM/UFF approach is the self-consistency of the charge distribution between the charge carrier and the environment so that polarization of both regions occurs. The QM/AMOEBA approach is less appealing in this respect because it neglects this interaction and instead relies on induced atomic dipoles for polarization.

Polarization effects due to solvent and crystal structure environment are often calculated using models where full solvation or embedding within a molecular crystal is represented as a dielectric continuum. Here, the polarization of a single-molecule charge carrier was calculated using the CPCM approach discussed in the Methodology. The CPCM polarization energy values would be comparable to those for infinite three-dimensional clusters treated with QM/MM methods; therefore, QM/UFF polarization energies of the finite-sized molecular clusters were used to extrapolate the polarization energies to infinite cluster sizes. Extrapolated QM/UFF polarization energies are reported in Table 2 for 2D single-layer and 3D clusters and the CPCM model. Both QM/UFF and CPCM calculations give the general trend that polarization energy decreases in magnitude with increasing molecular size, although the CPCM values are smaller in magnitude. The CPCM values for P_+ and P_- range from −1.48 to −1.10 eV for naphthalene through pentacene, respectively, while the values for infinite 3D QM/MM clusters range from −2.04 to −1.24 eV. However, since the CPCM model is an isotropic dielectric model, it gives identical or near-identical values for P_+ and P_-. Thus, QM/UFF again appears as a superior methodology that allows one to capture the subtle effects of molecular packing; this will be especially important when considering packing variations among polymorphs or within amorphous systems.

Table 2. Polarization Energies (in eV) of Oligoacenes[a] Calculated Using QM/MM and PCM Methods[b]

		B3LYP/UFF		B3LYP/AMOEBA		
		2D	3D	2D	3D	CPCM
$n = 2$	P_+	−1.56	−1.93	−1.21	−1.42	−1.48
	P_-	−2.21	−2.04	0.05	−0.69	−1.48
$n = 3$	P_+	−1.23	−1.76			−1.32
	P_-	−1.99	−1.83			−1.34
$n = 4$	P_+	−0.98	−1.35			−1.19
	P_-	−1.93	−1.73			−1.24
$n = 5$	P_+	−0.85	−1.24			−1.10
	P_-	−1.78	−1.49			−1.15

[a] n specifies the total number of fused benzene units. [b] QM calculations were performed at the B3LYP/6-31+G(d) level of theory.

d. Comparison to Experiment. There were several experimental values reported for polarization energies in oligoacene crystals and finite-sized clusters as determined by photoelectron spectroscopy.[1,11–15] Evaporated thin films of condensed polycyclic aromatic hydrocarbons with planar molecular structures were found to have a common P_+ value of 1.7 eV,[11] while P_- values were shown to be smaller in magnitude (which was explained to be due to counteracting total charge-quadrupole interactions for opposite charge carriers).[2,15] We note that there

is evidence that polarization energy strongly depends on crystal structure; P_+ for the α-crystalline form of perylene[64] was found to be 0.3 eV larger than that for β-perylene.[65]

As expected, molecular clusters increasing in size demonstrate corresponding increases in polarization energy. Factors such as the degree of disorder[14] and the spatial distribution[66,67] and location[68,69] of the excess charge within a cluster affect the polarization energies and experimentally observed vertical detachment energies. Coexisting disordered and crystal-like negative clusters of naphthalene and anthracene molecules were shown to exhibit different polarization energies,[14] and a larger spatial distribution of an excess charge was shown to give lower stabilization energy from polarization per neutral molecule.[67] Since charge distribution and order in cluster structures are difficult parameters to characterize experimentally, we focus below on localized charge carriers in perfectly crystalline structures as model systems.

Experimental values for the electronic polarization energies of naphthalene, anthracene, tetracene, and pentacene films were determined using expressions analogous to eq 2.[11,15] Reported experimental values of P_+ and P_- are in the range of −1.7 to −1.6 eV and −1.2 to −1.1 eV, respectively, for oligoacenes.[15] The values extrapolated from QM/UFF calculations on spherical clusters (Table 2) occur within a larger range of −1.9 to −1.2 eV for P_+ and −2.0 to −1.5 eV for P_-, and the asymmetry between P_+ and P_- is less pronounced and in the opposite direction than in the experimental values. For comparison, the QM/AMOEBA method gives a smaller value of $P_+ = -1.4$ eV for naphthalene due presumably to the neglect of charge redistribution. QM/UFF calculated P_- energies are 0.1−0.4 eV larger in magnitude than the P_+ energies, while QM/AMOEBA gives the opposite trend with P_- being ∼0.7 eV smaller in magnitude than P_+ for naphthalene. The CPCM continuum model gives P_+ values on the order of −1.5 to −1.1 eV and corresponding P_- values that are nearly identical, as expected from the isotropic nature of the dielectric continuum. Again, we emphasize that the advantage of the QM/MM approach is that molecular structure is explicitly taken into account, which will be especially important in studying materials that are amorphous or have particular structural defects. Charge redistribution within molecules was shown to contribute significantly to electronic polarization in organic molecular crystals.[17,18] The QM/UFF method allows charge to redistribute within the environment and gives magnitudes of polarization energy that are closer to experimental values than QM/AMOEBA.

The discrepancy between the QM/UFF results and the experimental data, in particular the narrow range of variation of $P_\pm$ as a function of oligomer size observed in experiment, suggests that in reality the charge carriers could be (de)localized over a similar number of carbons, irrespective of oligomer size. Work is in progress to better assess the relevance of this consideration and whether charge delocalization could be different for negative and positive carriers in crystalline materials.

On the basis of calculated values for charge-induced dipole and charge-quadrupole interactions and experimental estimates for relaxation energies,[20,70] Silinsh and co-workers[2,15] rationalized that P_+ and P_- differ because of asymmetry in the charge-quadrupole terms for different charge carriers. Tsiper and co-workers[17,18] used self-consistent equations to determine induced dipoles and molecular charge redistribution related to an atom−atom polarizability tensor. The QM/MM approach applied here builds on these works as it relies on a charge fluctuation model (QM/UFF) to capture the polarization energies in the oligoacene series.

B. Total Relaxation Energy in Naphthalene Crystals. The polarization energies calculated thus far contain only the electronic contributions that occur instantaneously upon charge carrier formation. Additional contributions to the total polarization energy come from intra- and intermolecular relaxations of the nuclear coordinates, or molecular and lattice polarizations, that occur on a considerably slower time scale.[2] Lattice relaxation energies in oligoacene crystals are expected to be small (∼0.01 eV) because of the rigidity of the crystal lattice.[2,71] The total polarization energy, W, associated with a charge carrier including contributions from electronic relaxation, that we denoted as $P_\pm$, as well as from nuclear relaxation, $L_\pm$, can be expressed according to eq 5. Decomposition of the total nuclear relaxation energy into contributions from the intramolecular nuclear relaxation of the localized charge carrier, $\lambda_{\pm,\text{internal}}$, and the nuclear relaxation of the environment due to electronic polarization, $\lambda_{\pm,\text{external}}$, is given in eq 6.

$$W_\pm = P_\pm + L_\pm \tag{5}$$

$$W_\pm = P_\pm + \lambda_{\pm,\text{internal}} + \lambda_{\pm,\text{external}} \tag{6}$$

The relaxation energies can be calculated directly from the adiabatic potential energy surfaces. The entire system in its neutral state is geometry-optimized to give energy $E_0(0)$ and the single-point energy of the optimized neutral geometry with a charge (that we take here, for the sake of example, to be positive) localized on a single naphthalene molecule is $E_0(+)$. The energy of the fully optimized charged system with the charge localized is $E_+(+)$. The total relaxation energy L_+ can then be calculated from the potential energy surface of the cation as $L_+ = E_0(+) - E_+(+)$. To determine $\lambda_{+,\text{external}}$, the geometry of the charged naphthalene molecule is frozen at the optimal neutral geometry and the geometries of the surrounding molecules are fully optimized to energy minimum $E_{+,\text{frozen}}(+)$. The value for $\lambda_{+,\text{external}}$ is the energy difference $E_{0,\text{frozen}}(+) - E_+(+)$ and is the reorganization energy of the environment due solely to electronic polarization. The contributions from $\lambda_{+,\text{internal}}$ can then be extracted using eqs 5 and 6.

The total relaxation energy, $L_\pm$, associated with the relaxation of both the molecule bearing the charge carrier and the surrounding molecules and lattice can be obtained with a QM/MM scheme. As an illustrative example, we considered two three-dimensional crystal structures of naphthalene molecules approximately 3 × 3 × 2 and 5 × 7 × 4 along the a, b, and c crystal directions. The total relaxation of the cation (L_+) embedded in the 3 × 3 × 2 cluster is 0.125 eV (B3LYP/6-31+G(d)/UFF) with 0.018 eV of the energy coming from relaxation of the environment, $\lambda_{+,\text{external}}$. The corresponding L_+ value for the 5 × 7 × 4 structure is 0.083 eV with $\lambda_{+,\text{external}} =$ 0.008 eV. In both cases, the relaxation energy of the surrounding

(64) Friedlein, R.; Crispin, X.; Suess, C.; Pickholz, M.; Salaneck, W. R. *J. Chem. Phys.* **2004**, *121*, 2239–2245.
(65) Friedlein, R.; Crispin, X.; Pickholz, M.; Keil, M.; Stafstrom, S.; Salaneck, W. R. *Chem. Phys. Lett.* **2002**, *354*, 389–394.
(66) Garcia, M. E.; Pastor, G. M.; Bennemann, K. H. *Phys. Rev. B: Condens. Matter Mater. Phys.* **1993**, *48*, 8388–8397.
(67) Bouvier, B.; Brenner, V.; Millie, P.; Soudan, J.-M. *J. Phys. Chem. A* **2002**, *106*, 10326–10341.
(68) Barnett, R. N.; Landman, U.; Cleveland, C. L.; Jortner, J. *J. Chem. Phys.* **1988**, *88*, 4429–4447.
(69) Makov, G.; Nitzan, A. *J. Phys. Chem.* **1994**, *98*, 3459–3466.
(70) Bounds, P. J.; Munn, R. W. *Chem. Phys.* **1981**, *59*, 41–45.
(71) Brovchenko, I. V. *Chem. Phys. Lett.* **1997**, *278*, 355–359.

molecules and lattice structure is small. The difference of 0.042 eV between the L_+ values is due to a greater amount of flexibility present in the smaller cluster.

The relaxation energy of the isolated naphthalene molecule corresponding to $\lambda_{+,\text{internal}}$ is 0.090 eV at the B3LYP/6-31+G(d) level of theory. Interestingly, $\lambda_{+,\text{internal}}$ of the $5 \times 7 \times 4$ cluster is smaller (0.075 eV) than that of the isolated molecule in the gas phase, while L_+ is closer (0.083 eV) to the gas-phase value. This suggests, at least for crystalline oligoacenes, that gas-phase reorganization energies of individual molecules may constitute reasonable approximations for total reorganization energies.

IV. Conclusions

We presented a quantum/classical computational strategy for calculating the polarization energy associated with the formation of a localized charge carrier in oligoacene crystals. Although discrepancies between calculated and experimental values exist, the present model qualitatively captures the magnitude of the polarization energy in oligoacenes, and its simplicity provides an efficient way to obtain parameters that are highly relevant for modeling charge transport in large systems, such as site energy distributions. This approach is general and can be applied to other organic crystals, amorphous solids, or polymer systems. Further refinement of the model can be achieved through the incorporation of additional polarizable force fields, self-consistent determination of both charge redistribution and induced dipoles, or the use of molecular dynamics or Monte Carlo simulation methods.

Importantly, we found that site energy differences, an important ingredient in the description of charge transport in organic materials, can be accurately determined from calculations on reasonably small molecular clusters. Also, we demonstrated that total reorganization energies associated with charge carrier formation are obtainable and provided evidence that lattice relaxation energies in oligoacenes are small.

The QM/MM methods reported here are now being extended to amorphous systems. Also, studies are currently underway to investigate the effects on polarization energies of the possibility of charge carrier delocalization on multiple molecules (various computational methods such as constrained DFT are being considered to investigate different degrees of charge delocalization in an ad hoc way, as at the present time there are no methods available to accurately determine charge delocalization in clusters of molecules of the size of naphthalene or larger). We hope that the theoretical results reported here will trigger new experimental work aimed at assessing in more detail the P_+ and P_- energies in oligoacenes and other π-conjugated organic semiconductors.

Acknowledgment. We acknowledge helpful and insightful discussions with Veaceslav Coropceanu, Hong Li, Indramil Rudra, and Demétrio A. da Silva Filho (Georgia Institute of Technology), Christian Lennartz (BASF Akteingesellschaft), and David Beljonne (University of Mons-Hainaut). This work was partly supported by BASF, the Office of Naval Research (under Grant N00014-04-1-0120), and the National Science Foundation (CRIF Program under Award CHE-0443564 and STC Program under Award DMR-0120967).

Supporting Information Available: Electronic energies for all the systems considered in this work (Tables S1−S14), a scheme illustrating the self-consistent charge equilibration process implemented for the QM/MM calculations (Scheme S1), and the complete ref 35. This material is available free of charge via the Internet at http://pubs.acs.org.

JA8017797